(NASA-TM-82081) GALACTIC γ-RAY EMISSION FROM PULSARS (NASA) 43 p HC A03/MF A01 CSCL 03B

N81-19999

Unclas
G3/93 18826

NASA

Technical Memorandum 82081

Galactic γ-Ray Emission from Pulsars

Alice K. Harding

JANUARY 1981

National Aeronautics and
Space Administration

Goddard Space Flight Center
Greenbelt, Maryland 20771

GALACTIC γ-RAY EMISSION FROM PULSARS

Alice K. Harding
Laboratory for High Energy Astrophysics
NASA/Goddard Space Flight Center

ABSTRACT

The contribution of pulsars to the γ-ray flux from the galactic plane is examined using data from the most recent pulsar surveys. It is assumed that pulsar γ-rays are produced by curvature radiation from relativistic particles above the polar cap and attenuated by pair production in the strong magnetic and electric fields. Assuming that all pulsars produce γ-rays in this way, their luminosities can be predicted as a function of period and magnetic field strength. The distribution of pulsars in the Galaxy is determined from data on 328 pulsars detected in three surveys. The Z and R distributions are very sensitive to the mean electron density in the galactic plane, as are the total number and birthrate of pulsars in the Galaxy.

The local γ-ray production spectrum for pulsars is steep above 100 MeV and is similar to the bremsstrahlung and Compton spectra. Longitude profiles of pulsar γ-ray flux are calculated for different values of the mean electron density. Because of the large center to anticenter flux ratio, pulsars contribute twice as much to the total flux toward the galactic center as they do toward the anticenter. The latitude profile is narrow, due to the fact that short period pulsars, which have the highest γ-ray luminosities, also have the smallest scale heights. The largest sources of uncertainty in the size of the pulsar contribution are the value of the mean interstellar electron density, the turnover in the pulsar radio luminosity function, and the average pulsar magnetic field strength. A present estimate is that pulsars contribute from 15-20 percent of the total flux of γ-rays from the galactic plane.

I. INTRODUCTION

The plane of our galaxy is the dominant source of high energy (> 100 MeV) γ-rays detected with the SAS-2 (Fichtel et al. 1975, Hartman et al. 1979) and COS-B (Paul et al. 1978, Mayer-Hasselwander et al. 1979) satellites. These observations have revealed, in some detail, the longitude and latitude dependent structure of the galactic γ-radiation. The large-scale emission shows a pronounced peak toward the galactic center between $\ell \approx 330^{\circ}$ and $\ell \approx 50^{\circ}$ and is relatively weak in the outer galaxy. The latitude profile is fairly narrow and falls off significantly within 10° of $b = 0^{\circ}$. On a finer scale, the emission shows spatial fluctuations, some of which may correspond to local or spiral arm features and all of which are smaller than the 1° resolution limit of the detectors. Two of these stand out strongly in the longitude profile and have been identified, through their timing signature, as the Crab and Vela pulsars. A number of other "point sources" of emission have been identified by COS-B (Wills et al. 1980), all of which have so far eluded definite identification with galactic sources at other wavelengths, although models and identifications have been proposed for some of the sources.

Diffuse emission processes which involve interactions between high energy cosmic rays and interstellar matter are considered to be a major source of galactic γ-rays. These processes include the decay of neutral pions produced in collisions between cosmic ray nucleons and interstellar gas nuclei, bremsstrahlung from cosmic ray electrons in the Coulomb fields of nuclei, and Compton scattering of microwave background and starlight photons from the cosmic ray electrons. The γ-ray emission, therefore, has great potential for revealing information on the origin and distribution of cosmic rays in the Galaxy and on the distribution of matter. Models for the galactic emission from diffuse processes using known distributions of CO and HI

(Stecker et al. 1975, Kniffen et al. 1977) require an increase in the cosmic ray density in the inner galaxy to explain the peak in γ-ray emission toward the galactic center, even with a large increase in molecular hydrogen density in the inner galaxy. This strongly suggests a galactic origin for most cosmic ray nuclei (Stecker 1975).

This picture, however, is complicated by the largely undetermined contribution from galactic point sources. Estimates have been made of the point source contribution using data on the COS-B sources (Protheroe et al. 1979, Bignami et al. 1978), but the estimates are uncertain due to a lack of knowledge of the distribution of these sources in the Galaxy. Without identification at other wavelengths, distance determination is impossible and thus the luminosities of these sources are also unknown. Another difficulty with this type of analysis is the inability to distinguish true point sources from enhancements in the spatial distribution due to diffuse processes.

At present, pulsars can give the best information on the galactic point source contribution. Since independent distance determinations can be made for pulsars via their dispersion measures, the galactic distribution of these objects is reasonably well known, except in the inner 3 kpc where statistics are poor. The Crab and Vela pulsars emit pulsed γ-rays and have been well studied by COS-B and SAS-2 (Bennett et al. 1977, Kniffen et al. 1974). Although a theoretical model for the acceleration of particles to energies high enough to produce the observed γ radiation has not been generally agreed upon, pulsars are certainly good candidates for high energy γ-ray sources on energetic grounds. Assuming that an efficient acceleration mechanism is operative, models for the production of γ-rays by primary particle curvature radiation, including the attenuation by pair production, are able to account for many of the observed

properties of the Crab and Vela pulsars (Harding et al. 1978, Salvati and Massaro 1978). Theory also suggests that all pulsars should be γ-ray emitters, with the γ-ray efficiency an increasing function of age and the shortest period pulsars having the highest luminosities (Harding 1981, Ayasli and Ögelman 1980). Furthermore, the predicted fluxes for the known radio pulsars indicate that many are right below the sensitivity threshold of the present γ-ray detectors.

Previous estimates have been made of the pulsar contribution to the γ-ray emission above 100 MeV. Higdon and Lingenfelter (1976) suggested that the contribution from unresolved pulsars could be as high as 40 percent, assuming that their γ-ray luminosities are directly proportional to their energy loss rates and that they have the same galactic distribution as the CO emission. Strong et al. (1977), assuming a direct proportionality between γ-ray and radio luminosity and using the distributions determined by Davies et al. (1977), concluded that the contribution would be no more than 5-10 percent. Neither of these estimates made use of a theoretical model for pulsar γ-ray emission and the large discrepancy in the results seems to indicate large uncertainties or errors in the assumptions made.

This paper makes a more thorough examination of the pulsar contribution and of the sources of uncertainty involved. We begin with a model for pulsar γ-ray production (§II) which can predict the luminosities as a function of pulsar parameters. All of the present data on radio pulsars is then used to determine the galactic distribution, taking into account the selection effects of the surveys (§III). In §IV, we estimate the pulsar contribution

to the local γ-ray emissivity and compare it to the production rates for various diffuse processes. Calculated longitude and latitude profiles are presented in §V and compared to the SAS-2 data. We conclude in §VI by discussing the major sources of uncertainty and the most reasonable present estimate of the pulsar contribution.

II. PULSAR γ-RAY LUMINOSITIES

The model we will use for the production of pulsar γ-rays is described in previous work (Harding et al. 1978, Harding 1981). It assumes that primary particles are accelerated to high energies in the magnetospheric electric fields and move along curved magnetic field lines, losing energy by generating curvature radiation γ-rays. The γ-rays which will be observed are those which escape conversion to electron-positron pairs in the strong pulsar magnetic field. The model takes into account rotation effects such as aberration, the electric field which is induced perpendicular to the magnetic field, and the rotation of the dipole field pattern in the frame of the photon. The shape of the calculated spectra depend on the initial energy of the primary particles, and on the pulsar magnetic field strength and period. A model with initial particle energy 1.5 X 10^{13} eV and field strength 10^{12} gauss gives a good fit to the observed spectra of both the Crab and Vela pulsars.

A general luminosity formula was derived and found to depend on the period P (in seconds) and the surface magnetic field strength B_{12} (in units of 10^{12} gauss) as:

$$L_\gamma(> 100 \text{ MeV}) = 1.2 \times 10^{35}\, B_{12}^{.95}\, P^{-1.7} \text{ photons s}^{-1}, \qquad (1)$$

which is normalized to give the correct luminosity for the Crab. This formula gives a value of L_γ(> 100 MeV) for Vela which is in good agreement with the observed value. Predicted luminosities for other pulsars give fluxes which, with the exception of a few, are all

below the upper limits given by SAS-2 (Ögelman et al. 1976). The few which are above the SAS-2 upper limits only exceed them by a factor of 2 or 3, which is not a serious discrepancy, considering that the errors in the limits are of the same magnitude. In addition, individual pulsar distances and magnetic field strengths can only be determined to within a factor of 2 or 3. The second COS-B catalog of point sources is now considered complete in the region $90^0 < \ell < 270^0$ down to a flux of 1.3 X 10^{-6} cm^{-2} s^{-1} (Swanenburg et al. 1981). Only two pulsars with predicted fluxes above this value lie in that longitude range and they are both located at high latitudes just outside the range of the search. None of the other pulsars have predicted fluxes exceeding the observed diffuse background level in their region of the sky. It seems that, at present, there are no serious discrepancies between what is predicted by the model and what is observed. Therefore, we will adopt the formula in equation (1) as a good estimate, on the average, of pulsar γ-ray luminosities, since we are concerned in this paper only with the collective properties of pulsar γ-ray emission in the Galaxy.

III. DISTRIBUTION OF PULSARS IN THE GALAXY

It is known from earlier statistical analyses that pulsars are distributed much like other Population I tracers in the Galaxy, such as ionized hydrogen, CO, and supernova remnants. The densities rise sharply toward the inner galaxy and fall off outside the solar circle. Previous analyses have been carried out on samples of 51 (Davies et al. 1977) 90 (Taylor and Manchester 1979), and 224 pulsars (Manchester 1979).

At present, there are 328 pulsars which have been detected in the various radio surveys. The three most sensitive searches, carried out at Arecibo (Hulse and Taylor 1974), Molonglo (Manchester et al. 1978) and NRAO (Damashek et.al. 1978), have collectively detected all the pulsars discovered in previous less sensitive surveys plus a substantial number of new ones. The entire galactic plane and all of the sky, except for the area south of $\delta = -85^{\circ}$, have been searched. In order to determine the galactic distribution from this sample of pulsars, one must take into account the selection effects of the surveys, which can be determined to reasonable accuracy.

We use the method described by Taylor and Manchester (1977, hereafter referred to as TM) to calculate the distribution of pulsars as a function of period P, height above the plane Z, galactocentric radius R, and radio luminosity L. The data on 328 pulsars used here is from Manchester and Taylor (1980). The number of pulsars detected in the intervals P to P + dP, Z to Z + dZ, R to R + dR and L to L + dL will be:

$$N_o (P,Z,R,L)dPdZdRdL = V(R,L)\rho(P,Z,R,L)dPdZdRdL \qquad (2)$$

where $V(R,L)$ is the effective volume of the Galaxy between Z and $Z + dZ$ and R and $R + dR$ searched for pulsars with periods between P and $P + dP$ and luminosities between L and $L + dL$. The true space density of pulsars in these same period and luminosity intervals is $\rho(P,Z,R,L)$. As TM have argued, the distributions with respect to P and Z are not seriously altered by selection effects, and there seems to be little observational correlation between L and P. Therefore, V depends only on R and L. If the distributions in P, Z, R, and L are independent, then the density may be expressed as:

$$\rho(P,Z,R,L) = \rho_P(P)N(Z)D(R)\rho_L(L). \tag{3}$$

The P and Z distributions, $\rho_P(P)$ and $N(Z)$, may be determined directly from the data without correcting for selection effects, while the R and L distributions will depend on $V(R, L)$.

a) Period Distribution

There is evidence of a correlation between the P and Z distributions for pulsars in the second Molonglo survey (Manchester 1979, Taylor 1979). Pulsars with longer periods tend to have larger scale heights which would be expected if they are born with large space velocities from a population having a small scale height. While this correlation will affect the latitude distribution of the galactic γ-ray flux from pulsars, it will not strongly affect the longitude profile, where we integrate over a latitude range which includes more than 2/3 of the pulsars. We will therefore treat $\rho_P(P)$ and $N(Z)$ as independent functions in computing the γ-ray longitude

profile, but take this correlation into account in [illegible]V in computing the latitude profile.

The period distribution for this sample of 328 pulsars is shown in Figure 1. The number falls off rather sharply at periods around 2s., which is well below the 3.9 s. long-period cutoff of all three surveys. The decrease in number of pulsars at short periods is also a real effect since the surveys were fully sensitive down to periods of .06s. The P distribution is therefore fairly narrow and peaks at periods between 0.5 and 1.0 s.

b. Pulsar Distances and the Interstellar Electron Density

The $\bar{Z}$ and $\bar{R}$ distributions depend strongly on the electron density distribution in the Galaxy, because pulsar distances are determined from their dispersion measures. If we assume an exponential dependence for the electron density,

$$n_e(z) = n_o \exp(-|z|/h_e), \tag{4}$$

then the distance to a pulsar with dispersion measure DM at galactic latitude b is given by

$$d = \frac{-h_e}{\sin|b|} \ln \left[1 - \frac{DM \sin|b|}{h_e n_o}\right]. \tag{5}$$

In the limit $b \rightarrow 0^o$, equation (5) approaches $d = DM/n_o$, so that the computed distance essentially varies inversely with n_o. Since pulsars are a disk

population, local densities will vary approximately as n_o^2. If one assumes that pulsars also have an exponential distribution,

$$N(z) = N_o \exp(-|z|/h_p), \qquad (6)$$

then the pulsar scale height, h_p will also depend strongly on n_o and weakly on the electron scale height, h_e, as long as $h_e >> h_p$.

The best estimates of the average n_o come from distance determinations to pulsars using measurements of the 21 cm. absorption of the pulsar signals by intervening hydrogen gas. From distance estimates for 32 pulsars and their dispersion measures, Weisberg et al. (1980) conclude that the mean interstellar electron density in the galactic plane on kiloparsec scales away from the galactic center region is 0.02-0.03 cm^{-3}. Although these is evidence for a longitude dependent variation in $<n_o>$ from this same data, we will assume that n_o is constant throughout the galactic plane. Within 1 kpc of the Sun, the clumpiness in the electron density distribution becomes important, and we take account of this by subtracting the contributions to the DM from nearby HII regions in the line of sight according to the method of Prentice and ter Haar (1969). The scale height of the electrons is less well determined, but it must be greater than the pulsar scale height or there would be a cutoff in DMsin|b|, the Z component of dispersion measure, which is not observed. We will assume that h_e = 1000 pc., which is the value adopted by TM, for the purpose of calculating distances.

c. Z and R Distributions

In light of the strong dependence of pulsar distances and densities on n_o,

the estimates of which are somewhat uncertain, we have determined the Z and R distributions for several possible values of n_o. Using the corrected dispersion measure data and h_e = 1000 pc., a least squares fit of equation (6) to the observed N(Z) distribution gives h_p = 400 ± 25 pc. for n_o = .02 cm^{-3}, h_p = 325 ± 20 pc. for n_o = .03 cm^{-3} and h_p = 230 ± 15 pc. for n_o = .04 cm^{-3}. These values are somewhat larger than the scale heights for n_o = .02 cm^{-3} and .03 cm^{-3} derived by TM, probably due to the greater number of long period, high Z pulsars detected in the second Molonglo survey which were not included in their sample.

In calculating the distribution of pulsars in galactocentric radius, we have divided the sample into those with $0^o \leq \ell < 180^o$ (positive longitudes) and those with $180^o \leq \ell < 360^o$ (negative longitudes). These two groups contain respectively 155 and 161 pulsars having measured fluxes at 400 MHz. We have used the iterative method described by TM to solve simultaneously for the R distribution and luminosity function for each group, assuming the Z distribution of equation (6) and semicircular symmetry about the galactic center. The R distributions for n_o = .03 cm^{-3}, in terms of the surface density of pulsars projected onto the galactic plane, are shown in Figure 2. The density scales were determined by integrating the derived luminosity functions to give the local surface densities. The most obvious feature at both positive and negative longitudes is a peak at around 5 kpc, where surface densities are five times greater than those at the Sun. The densities seem to fall off inside about 4 kpc, but the statistics are very poor and no firm conclusions can be made about pulsar densities in the inner galaxy. Even though D(10) at negative longitudes is about twice as large as at positive longitudes, the maximum densities near 5 kpc are very similar. The negative longitude distribution shows a secondary peak around 8 kpc and what appears to be a real deficit of pulsars between 6 and 7 kpc. These features are not present at positive

longitudes to any degree of significance. It is tempting to associate the secondary peak with the line of sight tangent to the Sagittarius arm which falls around 8 kpc. These distributions for $n_0 = .03$ cm^{-3} bear a striking resemblance to those of other Population I tracers. The 5 kpc peak in both ionized hydrogen (Lockman 1976) and CO emission, surveyed at positive longitudes only (Gordon and Burton 1976, Scoville and Solomon 1975), shows the same shoulder at 7.5 kpc and steep fall off at 4 kpc. as the pulsar distribution for $0 \leq \ell < 180^0$. The galactic γ-ray emissivity, determined by unfolding the SAS-2 longitude data (Stecker 1977, Caraveo and Paul 1979), peaks around 5 kpc at both positive and negative longitudes but also has a prominent secondary peak around 8 kpc at negative longitudes, thus showing the same type of asymmetry as the pulsars.

The R distribution changes drastically for other values of the mean electron density. The positive longitude distribution seems to be especially sensitive to the value of n_0 assumed. For $n_0 = .02$ cm^{-3}, the density increase toward the inner galaxy is much more gradual at both positive and negative longitudes. The 5 and 8 kpc peaks at negative longitudes shift inward and are less pronounced, while the structure at positive longitudes washes out completely, leaving no trace of a peak at 5 kpc. For $n_0 = .04$ cm^{-3}, the density increase is steeper and the structure which is present at $n_0 = .03$ cm^{-3} again tends to wash out. At negative longitudes there is only one peak and it appears between 6 and 7 kpc.

The greater sensitivity of the positive longitude distribution to changes in n_0, which are equivalent to changes in the distance scale, probably results from the way in which the observed pulsars are distributed.

At positive longitudes, the 5 kpc peak is mainly due to pulsars located between the Sun and the galactic center, where changes in distance result in large changes in R. Most of the structure in the negative longitude distribution is due to pulsars located along tangents to galactocentric circles, where changes in distance produce only small changes in R. Some, but not all, of this sensitivity to n_o at positive longitudes can be eliminated by removing the Arecibo pulsars from the sample. The Arecibo search was 10 times more sensitive than the others and confined to a small longitude range around $\ell = 40^o$.

d. Numbers and Birthrates

The total number of observable pulsars on each side of the Galaxy can be obtained by integrating over the R distributions:

$$N_G^{\pm} = \pi \int_0^{\infty} D^{\pm}(R) R dR. \tag{7}$$

The numbers calculated in this way for the different values of n_o are listed in Table 1. One would expect that, since the Sun is not in any preferred position in the Galaxy, N_G^+ and N_G^- would be equal. They turn out to be equal within the errors only for $n_o = .03\ cm^{-3}$, with $N_G^+ < N_G^-$ for $n_o = .02\ cm^{-3}$ and $N_G^+ > N_G^-$ for $n_o = .04\ cm^{-3}$. This result would seem to argue in favor of a mean electron density of $.03\ cm^{-3}$, and the argument is reinforced when one considers the shapes of the distributions for this value of n_o and their strong similarities to distributions of other Population I tracers in the Galaxy.

The total number of observable pulsars in the Galaxy for different n_o and the galactic birthrates which they imply are also listed in Table 1. The number $N_G = (3.7 \pm 0.6) \times 10^6$ for $n_o = .03\ cm^{-3}$ agrees with the number $N_G = (4.2 \pm 1.6) \times 10^6$ obtained by Manchester (1979), but is considerably greater than the result $N_G = (1.3 \pm 0.4) \times 10^6$ obtained by TM. If we assume that only 20 percent of pulsars are observable because of the beaming effect, and that their average lifetime is 10^7 year, which is probably an upper limit, then the galactic birthrate implied by this number is 1 every 5 years. Even considering the large uncertainties in this value, it would be inconsistent with the rate of occurrence of supernovae in the Galaxy if the rate were as small as 1 every 30 to 40 years (Milne 1979) or 1 every 80 years (Caswell and Lerche 1979).

IV. LOCAL γ-RAY PRODUCTION RATE

Using the results of §II and §III, we can determine the local γ-ray production rate for pulsars,

$$q^{\pm}_{psr}(>100\text{ MeV}) = \frac{D^{\pm}(10)}{2\,h_p} \int_0^{\infty} L_{\gamma}(P)\rho_P(P)dP, \tag{8}$$

where $D^{\pm}(10)$ is the surface density of pulsars at the Sun, h_p is the scale height, $L_{\gamma}(P)$ is the γ-ray luminosity formula given in equation (1) and $\rho_P(P)$ is the period distribution in Figure 1, normalized so that

$$\int_0^{\infty} \rho_P(P)dP = 1.$$

The value of q_{psr} (> 100 MeV) can then be compared to the local production rates which have been calculated for various diffuse processes. The luminosity $L_{\gamma}(P)$ also depends on the surface magnetic field strength as $B^{.95}$, so that q_{psr} (> 100 MeV) will be proportional to the <u>average</u> pulsar magnetic field strength. Since B cannot be measured directly, the only source of information on pulsar magnetic field strengths comes from measured slowdown rates and assumptions about neutron star structure. In view of this uncertainty, we will assume an average pulsar magnetic field strength of 10^{13} gauss in making these calculations, but remember that the results could scale up or down with a change in this value. The production rates calculated according to equation (8) for the different values of n_0 are shown in Table 2. The last column shows the fractional average production rate, $\langle q_{psr} \rangle / q_T = (q^{+}_{psr} + q^{-}_{psr})/2q_T$, assuming a total local emissivity of $q_T = 1.5\times10^{-25}$ cm^{-3} s^{-1}.

The differential production spectrum above 100 MeV can be calculated from the pulsar spectra predicted by the model discussed in §II. The characteristics of these spectra were described in an earlier paper (Harding 1981), where it was found that observed spectral data for both the Crab and Vela pulsars could be fit using the same parameters (except for the rotation period). If we assume that these parameters are valid for all pulsars, then their individual spectra will depend only on the period, and the differential production spectrum can be calculated using equation (8) with the intensity, $I_{\gamma}(P, E_{\gamma})$ in (photons s^{-1} MeV^{-1}) substituted for the luminosity $L_{\gamma}(P)$ and $\langle q_{psr} \rangle$ in place of $q^{\pm}_{psr}$. The resulting production spectrum for $n_0 = .03$ cm^{-3} is shown in Figure 3 along with production spectra which have been calculated by Stecker (1977) for the major diffuse processes. The calculated pulsar spectrum has been extrapolated below 100 MeV, although the model may not be accurate at the low energies due to the undetermined synchrotron contribution from secondary particles. The extrapolation thus represents a lower limit on the pulsar contribution below 100 MeV. Above 100 MeV and below 1 GeV, the pulsar spectrum is almost as steep as the bremsstrahlung and Compton spectra, and becomes steeper above 1 GeV due to the pair production and curvature radiation cutoffs. The pulsar production rate exceeds the "standard" production rate for electron bremsstrahlung calculated by Stecker up to about 2 GeV, and thus provides an additional source of emission which can steepen the total spectrum (Harding and Stecker 1980).

This steeper total spectrum is a better fit to the observed spectrum of the galactic emission than is the total spectrum from only diffuse processes. Figure 4 shows the total production spectrum of Figure 3 and the pulsar spectrum, which have been adjusted arbitrarily in magnitude to

fit the data points. There is no evidence in the data for a prominent peak at 70 MeV from π^0 decay, though the points cannot be fit by a straight power law either. It is interesting to note that the pulsar spectrum alone fits the data quite well, so that there are no spectral constraints in this model on the size of the pulsar contribution. In fact, pulsars could be a major source of the γ-ray emission below 100 MeV.

V. LONGITUDE AND LATITUDE PROFILES

The distribution of pulsar γ-ray flux in the Galaxy as a function of longitude and latitude may be determined from the local production rate and the galactic distributions, determined in §III. The flux from a given area of the sky $d\ell d\sin b$ will be

$$d\Phi(\ell,b)=\frac{q_{psr}}{4\pi}\int_0^\infty \rho_R(s,\ell,b)\, ds\, d\sin b\, d\ell, \tag{9}$$

where s is the distance along the line of sight and $\rho_R(s,\ell,b)$ is the pulsar density.

The flux at each longitude, integrated over a certain latitude range $b \leq b_{max}$, gives a longitude profile:

$$\frac{d\Phi(\pm\ \ell)}{d\ell} = \frac{q^{\pm}_{psr}}{4\pi}\int_{-b_{max}}^{b_{max}}\int_0^\infty \rho_R(s,\ \pm\ \ell,\ b)\, ds\, d\sin b. \tag{10}$$

The pulsar density is

$$\rho_R(s,\ \pm\ \ell,\ b) = \frac{D^{\pm}\{R(s,\ \ell)\}}{D^{\pm}(10)}\ N\{Z(s,b)\}, \tag{11}$$

where N(Z) is the exponential Z distribution given in equation (6) and $D^{\pm}(R)$ is the R distribution. The coordinate transformations between (R, Z) and (s, ℓ, b) are

$$\begin{aligned} Z &= s\ \sin b, \\ R &= (R_\theta^2 + r^2 - 2R_\theta\ r\ \cos\ell)^{\frac{1}{2}} \\ r &= s\ \cos b, \end{aligned} \tag{12}$$

where r is the distance s projected onto the plane and R_θ = 10 kpc is the distance of the Sun from the galactic center. If these expressions are used in equation (11) to determine the density at each point along the integration path, then equation (10) becomes:

$$\frac{d\Phi(\pm\ell)}{d\ell} = \frac{q^{\pm}_{psr}}{2\pi} h_p \int_0^{\infty} \frac{D^{\pm}\{R(r,\ell)\}}{D^{\pm}(10)} \{1 - \exp(^{-r \tan b_{max}/h_p})\} \frac{dr}{r} \quad (13)$$

We have numerically integrated this expression to obtain the γ-ray flux in 10^0 longitude bins over a latitude range $|b| \leq b_{max} = 10^0$, using a step size in r of 200 pc. The resulting profiles for the three values of electron density, n_o = .02, .03, and .04 cm^{-3}, are shown in Figure 5. The flux level increases as the mean electron density, and therefore the pulsar density, increases. The n_o = .03 and .04 profiles show sharp increases in flux between $\ell = 300^0$ and $\ell = 60^0$, with peaks in emission around $\ell = 30^0$ and $\ell = 330^0$. They are roughly symmetric around $\ell = 0^0$, although the flux decreases toward the anticenter more slowly at negative longitudes. The n_o = .02 profile is very asymmetric, with a much greater flux at negative longitudes. The large asymmetry in the R distribution for n_o = .02 was discussed in §III and it indicates that this value of n_o is probably too low.

These calculated profiles are plotted with the SAS-2 longitude data in Figure 6. The contribution from identified point sources has not been subtracted, but the strongest of these sources, including the Crab and Vela pulsars, are labeled. The calculated profiles are similar in shape to the observed profile , but they have a larger center to anticenter flux ratio. For n_o = .03 cm^{-3}, the pulsar contribution to the total flux

is 15 percent in the interval $300^{o} < \ell < 60^{o}$ which is about twice as large as the 7 percent contribution in the interval $60^{o} < \ell < 300^{o}$. For n_o = .04 cm^{-3}, the center contribution goes up to nearly 25 percent, while the anti-center contribution is around 10 percent. As mentioned in the last section, the pulsar γ-ray production rate scales with average magnetic field strength. Therefore, for an average surface field of say, 2×10^{12} gauss, the fluxes in Figure 6 would all be twice as large.

The latitude distribution of pulsar γ-ray flux can be calculated for a particular longitude or longitude range. Using equations (9), (11), and (12), we have

$$\frac{d\phi(\pm\ell,b)}{d\ell\ ds\mathrm{inb}} = \frac{1}{4\pi}\int_0^\infty D^{\pm}\{R(s,\ \ell)\}\int_0^\infty L_\gamma(P)\rho_p(P)\ \frac{1}{2h_p(P)}\ \exp\{-s|\sin b|/h_p(P)\}dPds. \tag{14}$$

Because of the dependence of scale height, h_p, on period as discussed in §III, the production rate is also a function of P and must appear under the integral along with the distribution functions. A least squares fit to the plot of average Z distance versus period for the pulsars in the Molonglo survey (Figure 2 of Taylor 1979) gives:

$$h_p(P) = 396\ P^{0.354}\ \mathrm{pc}. \tag{15}$$

The Z distances were calculated assuming that n_o = .03 cm^{-3} and h_e = 1000 pc. Using this relation in equation (14) produces the latitude distribution for

$\ell = 0^{0}$ shown in Figure 7. The profile is quite narrow due to the fact that the majority of γ-rays are produced by short period pulsars which have a relatively small scale height. At $\ell = 0^{0}$, most of these pulsars are at a distance of around 5 kpc, producing a distribution with a 2^{0} half-width. Because of the dependence of scale height on electron density, this width would be larger for $n_0 = .02\ cm^{-3}$ and smaller for $n_0 = .04\ cm^{-3}$. Since the pulsar latitude profile is so narrow, the size of the contribution to the total flux is not restricted by the small width of the observed latitude profile.

VI. DISCUSSION

We have presented a number of new results in this paper both on the distribution of pulsars in the Galaxy and on the pulsar contribution to diffuse galactic γ-rays. The pulsar R distribution is found to be significantly different at positive and negative longitudes. This difference may result from the spiral structure of the Galaxy if pulsars are located preferentially along spiral arms. The sensitive dependence of the distributions on mean electron density in the galactic plane provides a strong argument in favor of $n_0 = .03\ cm^{-3}$. This value is needed to give equal numbers of pulsars on both sides of the Galaxy and distributions which resemble those of other Population I objects.

The γ-ray flux contribution from pulsars in this model depends both on the number of pulsars in the Galaxy and on their average magnetic field strength. The two largest sources of uncertainty in the number of pulsars (as determined from the local surface density) are the mean electron density in the galactic plane and the minimum pulsar luminosity. The range in electron density we have considered, $.02\ cm^{-3} \leq n_0 \leq .04\ cm^{-3}$, represents about a factor of 3 uncertainty in the pulsar flux contribution. However, the arguement in § III (d) seems to rule out densities as low as $.02\ cm^{-3}$, so the range of possible values of n_0 is probably smaller. There is evidence that the electron density distribution is much more complex than the simple exponential model used here. The densities seem to be significantly higher in the inner Galaxy (Weisberg et al. 1980), suggesting an R dependence, and higher south of the galactic plane, suggesting a multicomponent Z distribution (Harding 1980). A model for the electron density incorporating these features could change the derived pulsar densities (Manchester 1980).

The local pulsar density derived for each value of n_0 depends critically on the lower limit chosen on the integral over pulsar radio luminosities. Due to the limited sensitivity of the searches, there are fewer low luminosity

pulsars in the sample and thus, some uncertainty in where the derived power law luminosity function turns over. However, a turnover is expected somewhere around the present sensitivity limit because the existence of many more pulsars in the Galaxy would only widen the gap between the pulsar birthrate and the supernova rate (cf. § III d).

Pulsar magnetic field strengths can be indirectly inferred from their slowdown rates. Although the rates of slowdown can be measured fairly accurately for many pulsars, a derivation of the surface magnetic fields requires a knowledge of neutron star radii and moments of inertia, which can only be determined by knowing the correct equation of state. The present theories of neutron star structure include a wide range of possible equations of state which predict a range of stable masses and radii (Baym and Pethick 1979). The range in these parameters gives a factor of 2 to 3 in average magnetic field strength, which gives the same uncertainty in the pulsar flux contribution. The range of average field strengths for a neutron star mass of 1.4 $M_\odot$ is roughly (0.7 - 1.6) x 10^{12} gauss, with the lower fields more likely for stiffer equations of state. The local γ-ray production rate from pulsars for n_0 = .03 cm^{-3} and an average field strength of 1 x 10^{12} gauss is 15 percent of the total production rate (cf. Table 2). This fraction could be anywhere from 10 to 25 percent from the above field strength range.

There are several characteristics of the galactic pulsar γ-ray flux which emerge regardless of the uncertainties. The production spectrum is as steep as the bremsstrahlung and Compton spectra above 100 MeV, although it is not a straight power law. The fact that the shape of the pulsar spectrum fits the observed galactic plane γ-ray spectrum quite well allows

the pulsar flux to be any fraction of the total emission. The shape of a pure π^0 decay spectrum does not fit the COS-B spectral data points (Paul et al. 1978), placing an empirical upper limit to the fraction which π^0 decay can contribute to the total emission. Several authors (Cesarsky et al. 1978, Strong et al. 1978, Hartman et al. 1979) have concluded that large bremsstrahlung contributions are needed to give total spectra which fit the shape of the observed γ-ray spectrum. The size of these contributions requires a flux of cosmic ray electrons which is from 2 to 5 times higher than what is expected from the observed electron flux at the Earth, after correcting for solar modulation. In addition, the ratio of bremsstrahlung flux to π^0 decay flux needed requires much higher electron to proton ratios than are observed near the Sun. Pulsars provide an additional steep spectrum source of emission which has not previously been included in analyses of the galactic γ-ray spectrum. With the pulsar contribution included, a good fit to the spectral data can be obtained with a lower bremsstrahlung contribution and thus, lower electron fluxes and electron to proton ratios.

We have also found that the pulsar flux percentage contribution is twice as large toward the galactic center as it is toward the anticenter. The diffuse flux component, which is the difference between the total flux and the point source flux, will then have a smaller center to anticenter ratio than the total flux. The cosmic ray density variation in the Galaxy needed to explain the total flux increase toward the galactic center could therefore be smaller. The latitude distribution of the pulsar flux is quite narrow and, in fact, has a smaller width than the observed latitude distribution of γ-ray flux toward the galactic center (which may be resolution limited). We have obtained this result by using recent direct evidence that short period pulsars, predicted to be the most luminous γ-ray emitters, have a

smaller scale height, comparable to their Population I progenitors. Studies of the diffuse galactic γ-ray spectrum at high latitudes (Fichtel et al. 1978; Lebrun and Paul 1979) also show the significant low energy excess seen at low latitudes, requiring a steep spectral contribution greater than the "standard" bremsstrahlung component. From Figure 7, the estimated pulsar flux is about 10 percent of the galactic flux at $b \sim 15^{\circ}$, given by Fichtel et al. to be $(4.0 \pm 1.0) \times 10^{-5}$ cm^{-2} s^{-1} sr^{-1}. Even at these higher latitudes, then, pulsars could supply some of the steep spectral contribution that is needed. This high latitude contribution would come primarily from older pulsars, individually weak as γ-ray sources, and therefore consistent with the absence of strong high latitude point sources.

In estimating the pulsar contribution, we have counted only observable radio pulsars as sources of γ-ray emission. It is possible that there exists a population of pulsars emitting pulsed γ-rays but no pulsed radio emission. In the γ-ray pulsar model considered in this paper, the shortest period pulsars have the highest luminosities. If there are long period pulsars which turn off in the radio before turning off at γ-ray energies, they would not be luminous enough to contribute much to the galactic emission. If, however, there are short period pulsars which have turned on at γ-ray energies prior to turning on in the radio, then these objects could be contributing as much as the radio luminous pulsars to the galactic emission. Michel (1978) predicts that incoherent radiation makes up an increasingly greater fraction of the total available energy as pulsar period decreases. Since observable radio emission requires a coherent process, pulsars with extremely short periods could be under luminous in the radio but very luminous in γ-rays.

In summary, the present estimate of a 15 percent to 20 percent pulsar contribution to the total γ-ray emission in the Galaxy represents only the contribution from conventional radio pulsars. It indicates that the total contribution from all point sources of γ-ray emission could be substantial and should not be overlooked in considering models for diffuse processes and cosmic rays.

The author would like to thank F. W. Stecker and D. J. Thompson for extremely useful discussions and suggestions, and J. H. Taylor and P. R. Backus for supplying up-to-date pulsar data.

REFERENCES

Ayasli, S. and Ögelman, H. 1980, Ap. J., 237, 227.

Baym, G. and Pethick, C. J. 1979, Ann. Rev. Astron. Astrophys., 17, 415.

Bennett, K. et al., Astron. Astrophys., 61, 279.

Bignami, G. F., Caraveo, P. and Maraschi, L. 1978, Astron. Astrophys., 67, 149.

Bignami, G. F., Fichtel, C. E., Kniffen, D. A. and Thompson, D. J. 1975, Ap. J., 199, 54.

Caraveo, P. A. and Paul, J. A. 1979, Astron. Astrophys., 75, 340.

Caswell, J. L. and Lerche, I. 1979, M. N. R. A. S., 187, 201.

Cesarsky, C. J., Paul, J. A. and Shukla, P. G. 1978, Astrophys and Sp. Sci., 59, 73.

Damashek, M., Taylor, J. H. and Hulse, R. A. 1978, Ap. J. (Letters), 225, L31.

Davies, J. G., Lyne, A. G. and Seiradakis, J. H. 1977, MNRAS, 179, 635.

Fichtel, C. E., Hartman, R. C., Kniffen, D. A., Thompson, D. J., Bignami, G. F., Ögelman, H. B., Özel, M. E. and Tümer, T. 1975, Ap. J., 198, 163.

Fichtel, C. E., Simpson, G. A. and Thompson, D. J. 1978, Ap. J., 222, 833.

Gordon, M. A. and Burton, W. B. 1976, Ap. J., 208, 346.

Harding, A. K. 1980, Pulsars, ed. W. Sieber and R. Wielebinski (Dordrecht: Reidel), in press.

Harding, A. K. 1981, Ap. J., in press.

Harding, A. K. and Stecker, F. W. 1980, Nature, submitted.

Harding, A. K., Tademaru, E. and Esposito, L. W. 1978, Ap. J., 225, 226.

Hartman, R. C., Kniffen, D. A., Thompson, D. J., Fichtel, C. E., Ögelman, H. B., Tümer, T. and Özel, M. E. 1979, Ap. J., 230, 597.

Higdon, J. C. and Lingenfelter, R. E. 1976, Ap. J. (Letters), 208, L107.

Hulse, R. A. and Taylor, J. H. 1974, Ap. J. (Letters), 191, L59.

Kniffen, D. A., Fichtel, C. E. and Thompson, D. J. 1977, Ap. J., 215, 765.

REFERENCES (Cont'd.)

Kniffe , D. A., Hartman, R. C., Thompson, D. J., Bignami, G. F., Fichtel, C. E., Ögelman, H. B. and Tümer, T. 1974, Nature, 251, 397.

Lebrun, F. and Paul, J. A. 1979, Proc. 16th Int. Cosmic Ray Conf., 12, 13.

Lockman, F. J. 1976, Ap. J., 209, 429.

Manchester, R. N. 1979, Aust. J. Phys., 32, 1.

Manchester, R. N. 1980, private communication.

Manchester, R. N., Lyne, A. G., Taylor, J. H., Durdin, J. M., Large, M. I. and Little, A. G. 1978, MNRAS, 185, 409.

Manchester, R. N. and Taylor, J. H. 1980, A. J., in press.

Mayer-Hasselwander et al., 1979, Ann. N. Y. Acad. Sci., in press.

Michel, F. C. 1978, Ap. J., 220, 1101.

Milne, D. K. 1979, Aust. J. Phys., 32, 83.

Ögelman, J. B., Fichtel, C. E., Kniffen, D. A. and Thompson, D. J. 1976, Ap. J., 209, 584.

Paul, J. A. et al. 1978, Astron. Astrophys., 63, L31.

Prentice, A. J. R. and ter Haar, D. 1969, MNRAS, 146, 423.

Protheroe, R. J., Strong, A. W., Wolfendale, A. W. and Kiraly, P. 1979, Nature, 277, 542.

Salvati, M. and Massaro, E. 1978, Astron. Astrophys., 67, 55.

Scoville, N. Z. and Solomon, P. M. 1975, Ap. J. (Letters), 199, L105.

Stecker, F. W. 1975, Phys. Rev. Letters, 35, 188.

Stecker, F. W. 1977, Ap. J., 212, 60.

Stecker, F. W. 1979, Ap. J., 228, 919.

Stecker, F. W., Solomon, P. M., Scoville, N. A. and Ryter, C. E. 1975, Ap. J., 201, 90.

Strong, A. W., Wolfendale, A. W., Bennett, K. and Wills, R. D. 1978, MNRAS, 182, 751.

REFERENCES (Cont'd.)

Strong, A. W., Wolfendale, A. W. and Dahanayake, C. 1977, MNRAS, 179, 69.

Swanenburg, B. N. et al. 1981, Ap. J. (Letters), in press.

Taylor, J. H. 1979, The Large-Scale Characteristics of the Galaxy, ed. W. B. Burton (Dordrecht: Reidel), p. 119.

Taylor, J. H. and Manchester, R. N. 1977, Ap. J., 215, 885.

Weisberg, J. M., Rankin, J. and Boriakoff, V. 1980, Astron Astrophys., 88, 84.

Wills, R. D. et al. 1980, Non-Solar Gamma-Rays (COSPAR), ed. R. Cowsik and R. D. Wills (New York: Pergamon), 43.

TABLE 1

PULSAR SCALE HEIGHTS, DENSITIES, AND IMPLIED BIRTHRATES

MEAN ELECTRON DENSITY	SCALE HEIGHT	LOCAL PULSAR DENSITY (kpc^{-2})		OBSERVABLE NUMBER (10^6)			IMPLIED BIRTHRATE a)
n_o (cm^{-3})	h_p(pc.)	$D^+(10)$	$D^-(10)$	N_G^+	N_G^-	N_G	
.02	400 ± 25	170 ± 30	294 ± 50	0.65 ± 0.11	1.4 ± 0.2	2.1 ± 0.3	0.1 yr^{-1}
.03	325 ± 20	290 ± 50	564 ± 81	1.8 ± 0.3	1.9 ± 0.3	3.7 ± 0.6	0.2 yr^{-1}
.04	230 ± 15	432 ± 64	825 ± 105	2.9 ± 0.4	2.0 ± 0.3	4.9 ± 0.7	0.25 yr^{-1}

a) Beaming factor of 20 percent and an average pulsar lifetime of 10^7 year assumed.

TABLE 2

LOCAL PULSAR γRAY PRODUCTION RATES ABOVE 100 MeV

MEAN ELECTRON DENSITY	LOCAL PRODUCTION RATES		FRACTION OF TOTAL EMISSIVITY
$\langle n_o \rangle$ (cm^{-3})	q^{+}_{psr} (photons cm^{-3} s^{-1})	q^{-}_{psr} (photons cm^{-3} s^{-1})	$\langle q_{psr} \rangle / q_T$ a)
.02	$(6.3 \pm 1.6) \times 10^{-27}$	$(1.1 \pm 0.3) \times 10^{-26}$	.06
.03	$(1.5 \pm 0.3) \times 10^{-26}$	$(2.9 \pm 0.5) \times 10^{-26}$	.15
.04	$(2.8 \pm 0.6) \times 10^{-26}$	$(5.3 \pm 1.0) \times 10^{-26}$	.27

a) Assuming a total local emissivity above 100 MeV, $q_T = 1.5 \times 10^{-25}$ photons cm^{-3} s^{-1}.

FIGURE CAPTIONS

Figure 1--Period distribution of the observed pulsars.

Figure 2--Surface density of pulsars versus galactocentric radius at positive and negative longitudes for a mean electron density, $n_0 = .03\ cm^{-3}$.

Figure 3--Differential production spectrum for pulsars with an average magnetic field strength of 10^{12} gauss, for a mean electron density $n_0 = .03\ cm^{-3}$. Production spectra for diffuse processes are from Stecker (1977). The high energy part of the π^0 spectrum is from Stecker (1979).

Figure 4--Total spectrum and pulsar spectrum from Figure 3 fit to the data points from SAS2 and COSB for $355^0 < \ell < 15^0$.

Figure 5--Pulsar γ-ray flux longitude profiles for different values of the mean electron density in cm^{-3}.

Figure 6--Longitude profiles from Figure 5 plotted with the SAS2 longitude flux from Hartman et al. 1979.

Figure 7--Latitude profile of pulsar flux at $\ell = 0^0$ for $n_0 = .03\ cm^{-3}$.

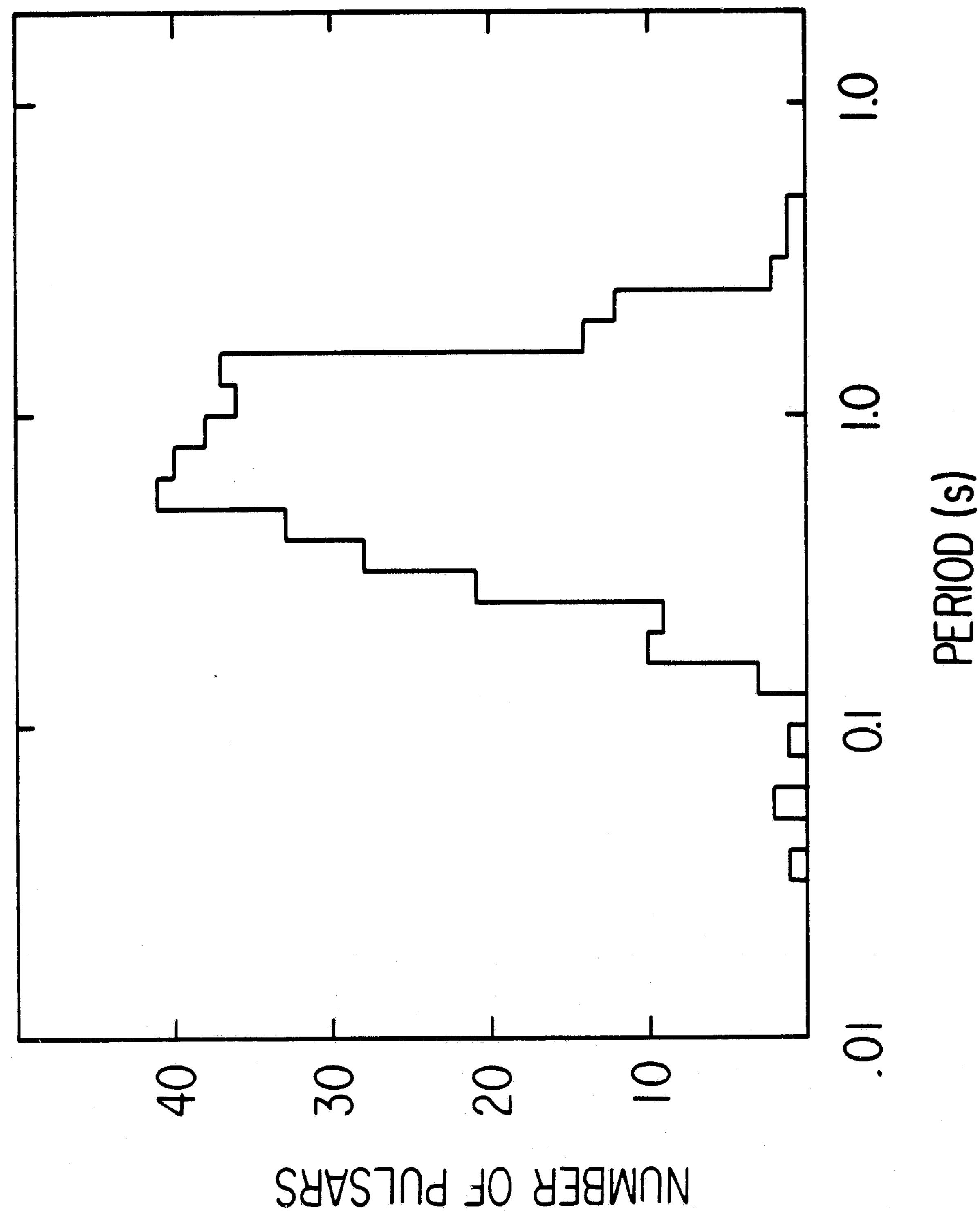

Figure 1

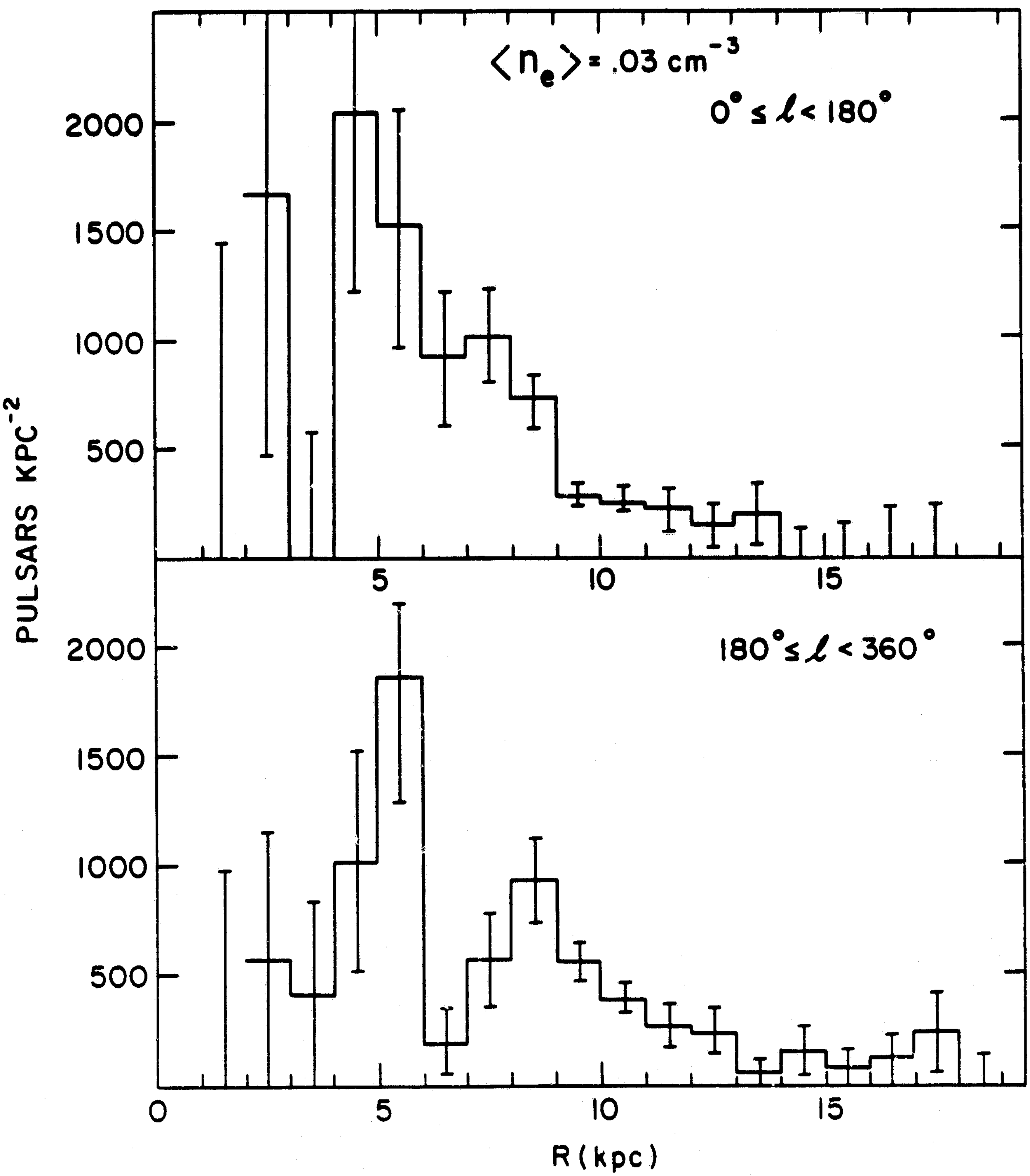

⟨n_e⟩ = .03 cm^-3
0° ≤ ℓ < 180°
180° ≤ ℓ < 360°
2000
1500
1000
500
PULSARS KPC^-2
0
5
10
15
R (kpc)

Figure 2

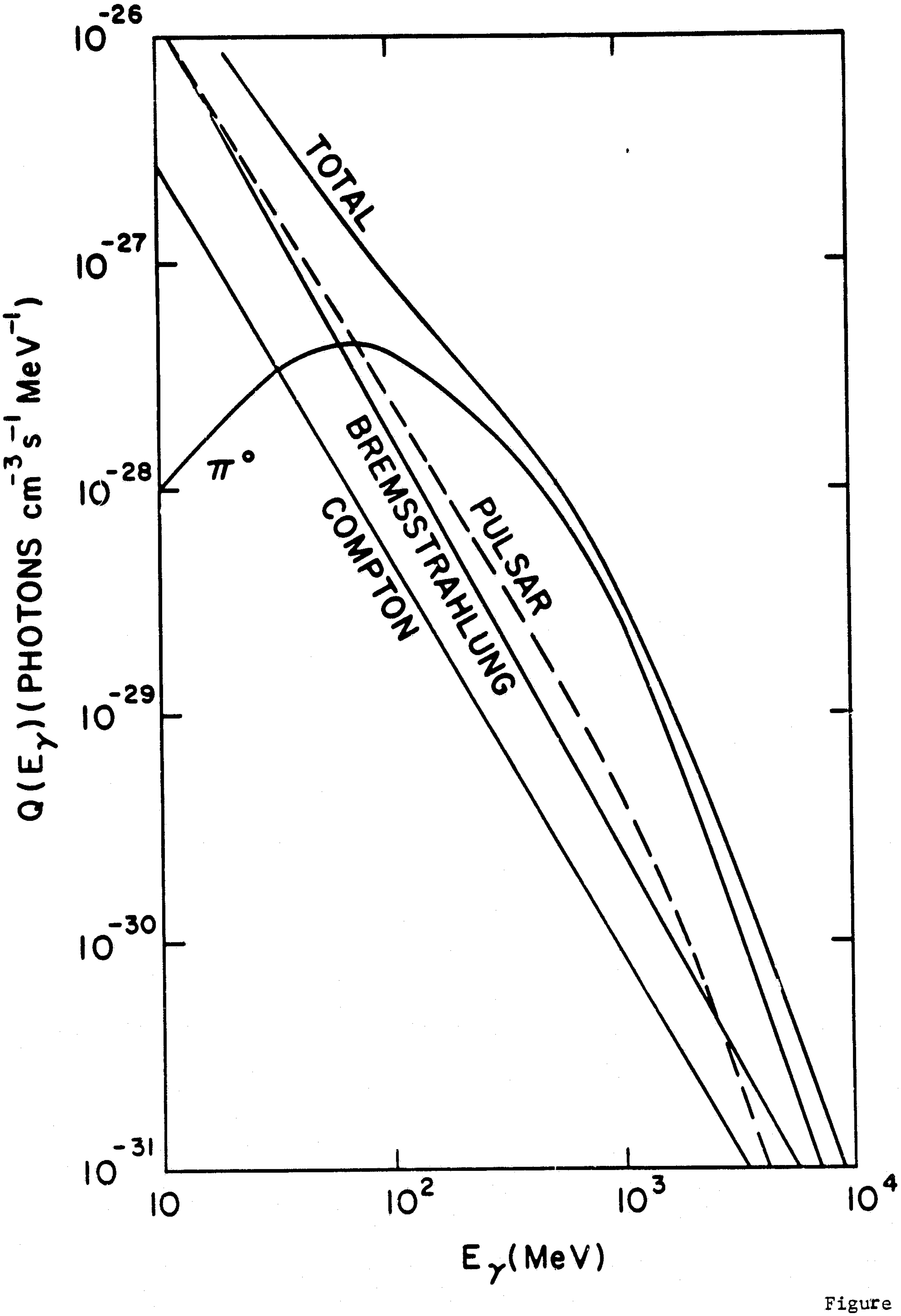

10^{-26}
10^{-27}
10^{-28}
10^{-29}
10^{-30}
10^{-31}
10
10^2
10^3
10^4
$Q(E_\gamma)$ (PHOTONS $cm^{-3}s^{-1}MeV^{-1}$)
E_γ(MeV)
TOTAL
π°
BREMSSTRAHLUNG
PULSAR
COMPTON

Figure 3

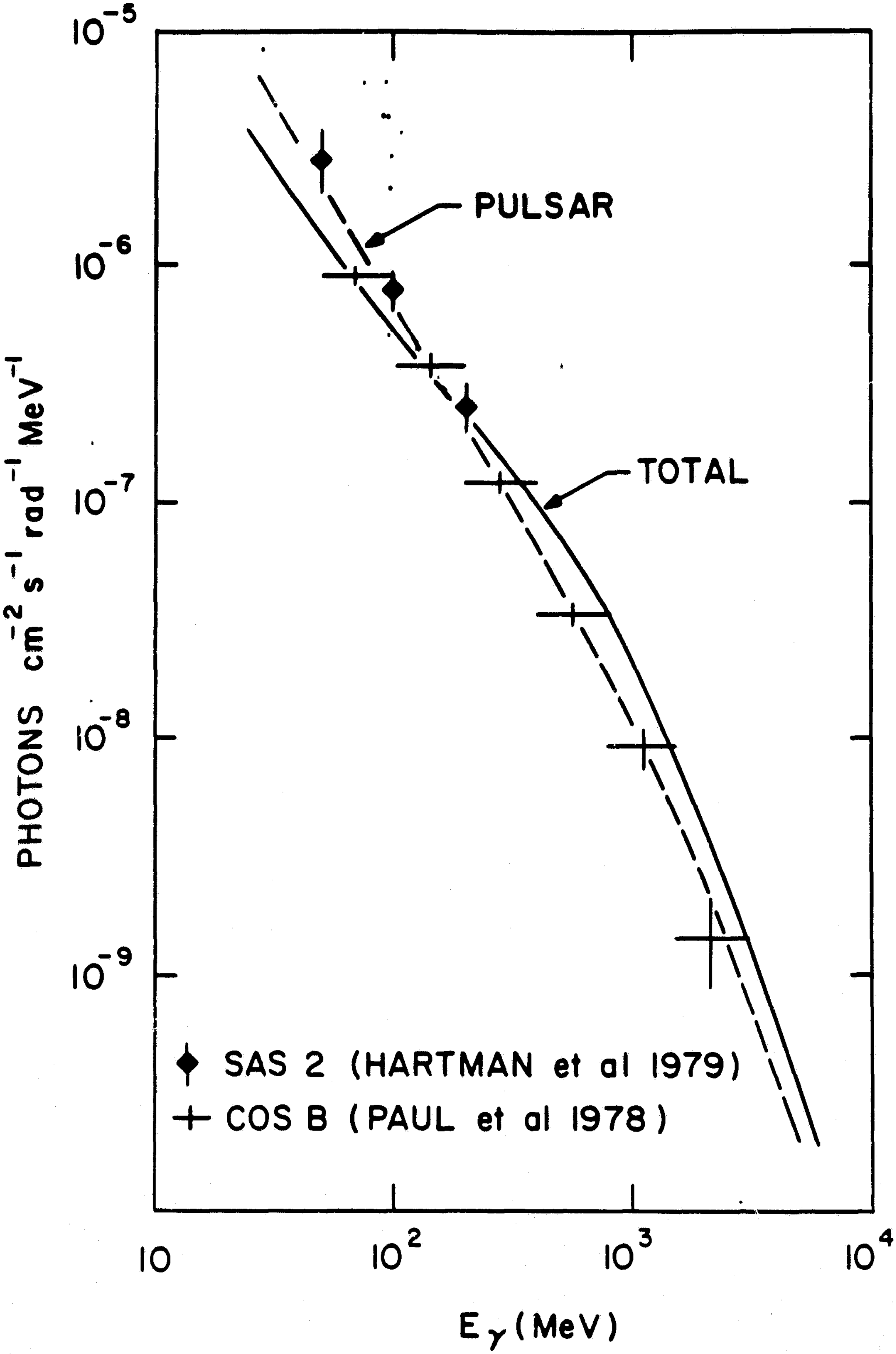

PULSAR
TOTAL
PHOTONS $cm^{-2} s^{-1} rad^{-1} MeV^{-1}$
10^{-5}
10^{-6}
10^{-7}
10^{-8}
10^{-9}
SAS 2 (HARTMAN et al 1979)
COS B (PAUL et al 1978)
10
10^2
10^3
10^4
E_γ (MeV)

Figure 4

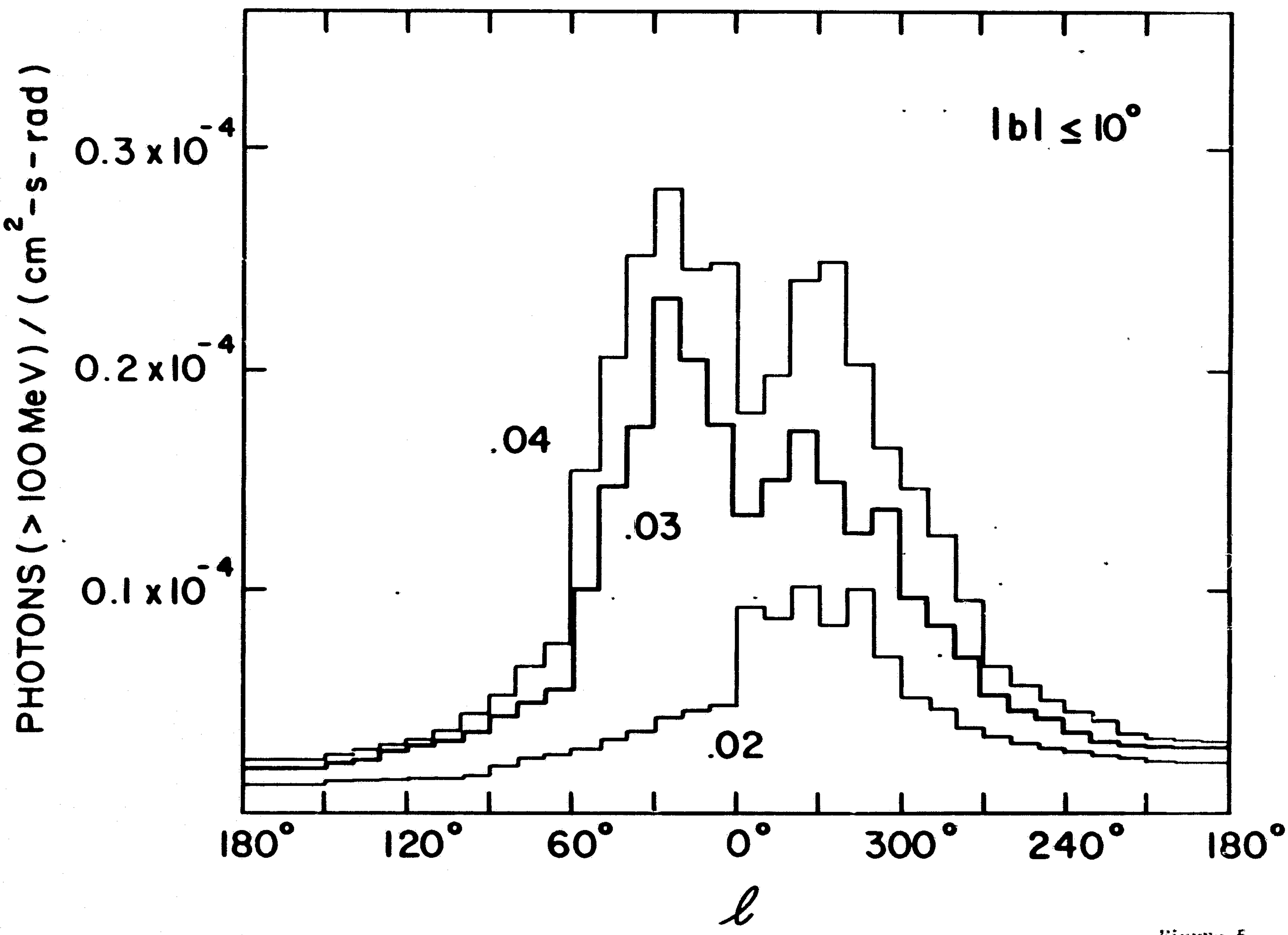

PHOTONS (> 100 MeV) / (cm^2-s-rad)
0.3 x 10^{-4}
0.2 x 10^{-4}
0.1 x 10^{-4}
|b| ≤ 10°
.04
.03
.02
180°
120°
60°
0°
300°
240°
180°
ℓ

Figure 5

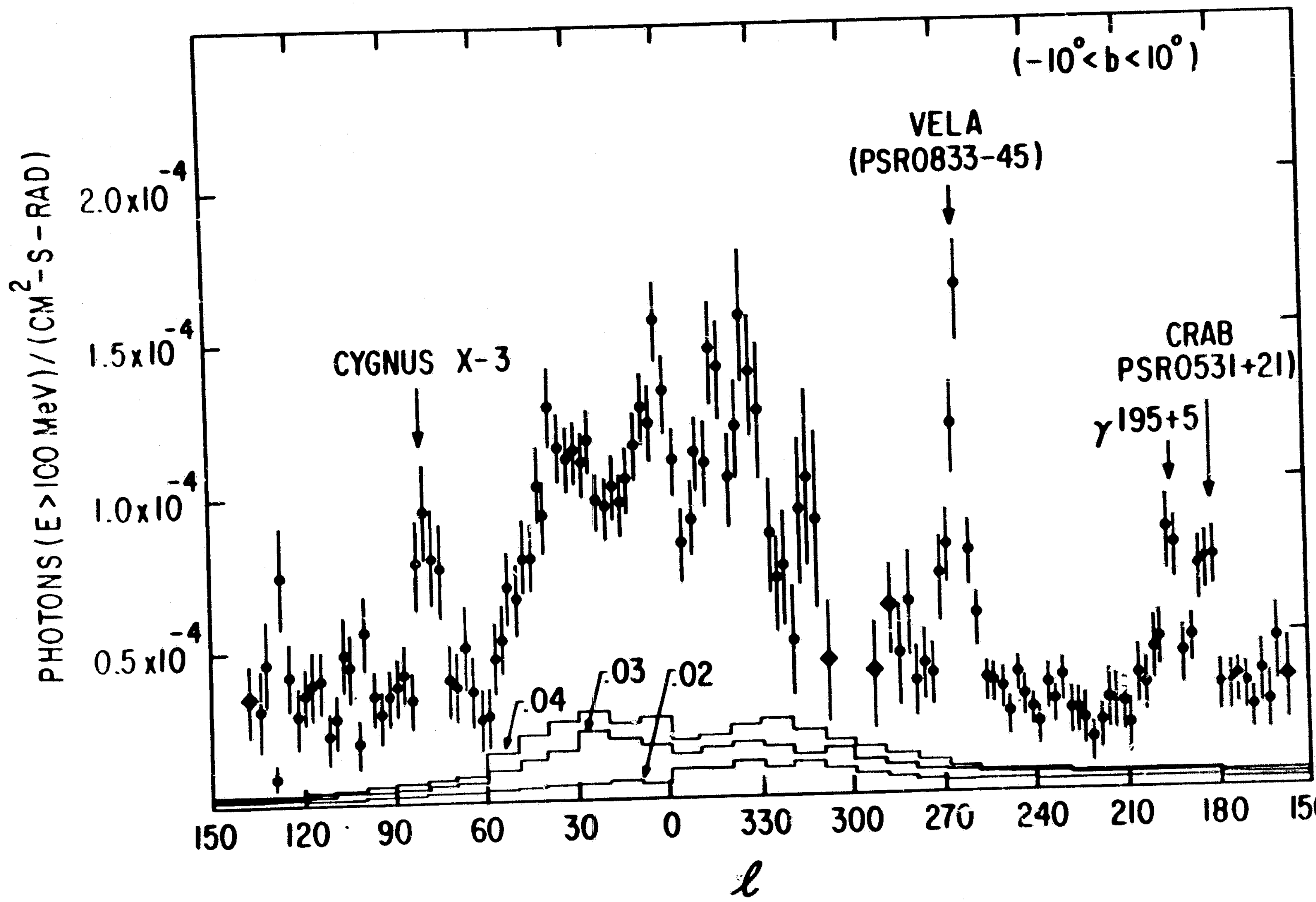

(−10° < b < 10°)
VELA
(PSR0833−45)
CRAB
PSR0531+21)
γ 195+5
CYGNUS X-3
PHOTONS (E > 100 MeV)/(CM²-S-RAD)
2.0x10⁻⁴
1.5x10⁻⁴
1.0x10⁻⁴
0.5x10⁻⁴
.04
.03
.02
150
120
90
60
30
0
330
300
270
240
210
180
150
ℓ

Figure 6

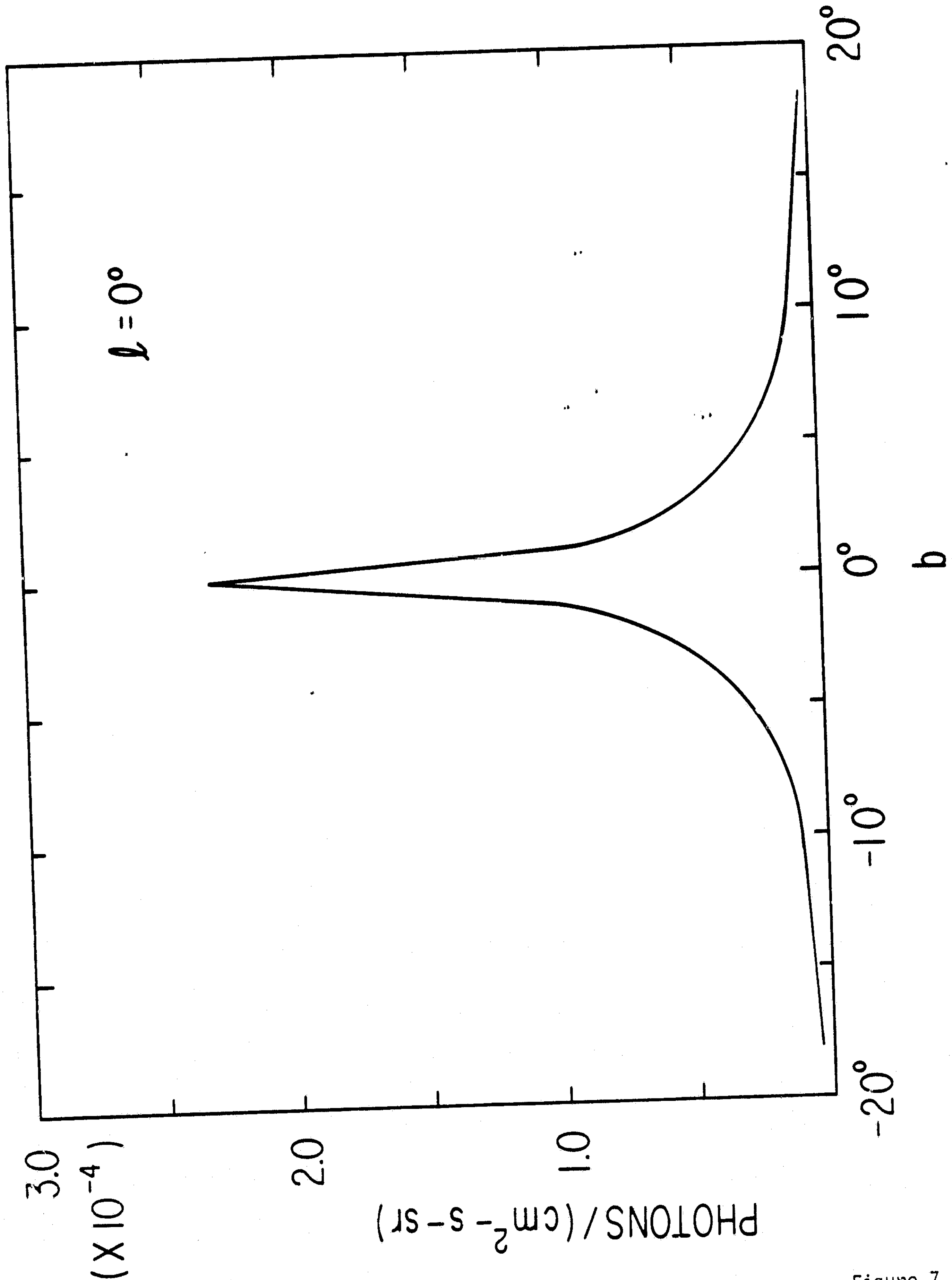

Figure 7